Exp Fluids
DOI 10.1007/s00348-011-1165-4

RESEARCH ARTICLE

Turbulence measurements in pipe flow using a nano-scale thermal anemometry probe

M. Vallikivi · M. Hultmark · S. C. C. Bailey · A. J. Smits

Received: 14 February 2011 / Revised: 16 June 2011 / Accepted: 1 July 2011

Abstract A new nano-scale thermal anemometry probe (NSTAP) has been developed using a novel procedure based on deep reactive ion etching. The performance of the new probe is shown to be superior to that of the previous design by Bailey (J Fluid Mech 663:160–179, 2010). It is then used to measure the streamwise velocity component of fully developed turbulent pipe flow, and the results are compared with data obtained using conventional hot-wire probes. The NSTAP agrees well with the hot-wire at low Reynolds numbers, but it is shown that it has better spatial resolution and frequency response. The data demonstrate that significant spatial filtering effects can be seen in the hot-wire data for probes as small as 7 viscous units in length.

1 Introduction

The spectral content of turbulence provides the basis for many theories of turbulence, including the famous result of Kolmogorov, who showed that at sufficiently high Reynolds number, the spectrum is expected to show a region with a slope of $k^{-5/3}$, where k is the magnitude of the wavenumber integrated over all directions (Kolmogorov 1941). This region is called the inertial region and corresponds to the transfer of energy from the energy-containing motions to the energy-dissipating motions. In a wall-bounded flow, such as fully developed turbulent pipe flow, this scaling may be deduced by an overlap argument in spectral space between a region that scales on y, the distance from the wall, and one that scales with η, the Kolmogorov length scale (Perry et al. 1986). A similar overlap argument between the motions that scale on y and the flow-dependent motions that scale on R, where R is a measure of the shear layer thickness such as the pipe radius, leads to a k^{-1} scaling. More recently, observations of the low-wavenumber spectrum have led to the identification of the very large-scale motions in pipe flow (Kim and Adrian 1999), and studies on the dissipation spectrum have revealed the universality (i.e., Reynolds number independence) of the dissipating motions and shown that significant dissipation occurs at scales as large as 10η (Bailey et al. 2009).

The experimental evidence supporting these concepts is usually based on frequency spectra obtained using hot-wire anemometry. Indeed, one of the principal reasons why hot-wire anemometry continues to be an important tool in turbulence research is because it gives a continuous time signal, making it possible to construct frequency spectra. However, the hot-wire anemometer suffers from limitations on spatial resolution, in that it may not be able to resolve the full range of scales, particularly the smallest motions. It may also have insufficient temporal resolution, in that its frequency response may be inadequate to follow the highest frequency fluctuations. These limitations have been the subject of much previous work (see, for example, Ligrani and Bradshaw 1987 and Comte-Bellot 1976), suggesting that hot-wire probes will produce reliable statistics when the non-dimensional wire length $l_w^+ \leq 20$ (where $l_w^+ = l_w u_\tau / \nu$, l_w is wire length, $u_\tau = \sqrt{\tau_w/\rho}$ is friction velocity, τ_w is wall shear stress and ν is kinematic

M. Vallikivi (✉) · M. Hultmark · A. J. Smits
Department of Mechanical and Aerospace Engineering, Princeton University, Princeton, NJ 08544, USA
e-mail: mvalliki@princeton.edu

S. C. C. Bailey
Department of Mechanical Engineering, University of Kentucky, Lexington, KY 40506, USA

Published online: 21 July 2011

viscosity). Recent studies have emphasized the effects of spatial resolution on measuring the magnitude of the near-wall peak in the variance of the streamwise velocity component, $\overline{u^2}$, in wall-bounded turbulence (Hutchins et al. 2009 and Hultmark et al. 2010), while Smits et al. (2011) have proposed a comprehensive correction method for the effects of spatial filtering on $\overline{u^2}$ for all wall distances. In addition, Chin et al. (2009) used DNS data to formulate an empirical model of the missing streamwise component energy spectra as a function of wire length, and Cameron et al. (2010) studied the effect of anisotropy on the measurements of spectra using finite-length wires.

However, any correction scheme must rely to some extent on known or predictable behavior, a bias that needs to be avoided when investigating new phenomena. There is a clear need for an instrument that has sufficient spatial and temporal resolution to measure turbulent fluctuations accurately over the entire spectrum, especially at high Reynolds number. To help achieve that aim, Bailey et al. (2010) designed and tested a nano-scale thermal anemometry probe (NSTAP) that is an order of magnitude smaller than conventional hot-wire probes and displays a considerably higher frequency response. Their design, shown in Fig. 1, has a 60-μm-long sensing element, measuring 100 nm by 2 μm in cross section, with a frequency response that exceeds 150 kHz when operated in the constant temperature mode. A study of grid turbulence demonstrated that this original NSTAP behaved similar to conventional hot-wire probes but with better spatial resolution and improved temporal response, allowing investigation into spatial resolution effects on higher-order moments and velocity increment statistics.

Two shortcomings of the probe used by Bailey et al. (2010) were the fabrication difficulties and its rather blocky design. As can be seen from Fig. 1, the shape of the probe tip was not particularly streamlined, primarily because the probe shape was formed by laser machining, which is not precise enough to manufacture a better supporting structure. As a result of aerodynamic interference between the supports and the sensing element, the probe was sensitive to the effects of pitch, as shown in Fig. 2 (hollow symbols), which made it unsuitable for measurements in regions of high turbulence intensity such as those found in the near-wall region of wall-bounded flows. The effects of the pitch sensitivity were most noticeable in the logarithmic region, where the NSTAP consistently overestimated the turbulence intensities.

Here, we describe the design and construction of a more streamlined NSTAP that is much less sensitive to pitch (see Fig. 2, filled symbols) and performs well in wall-bounded flows. This probe was then used in the study of turbulent spectra in fully developed pipe flow for Reynolds numbers (Re_D) of 45×10^3, 80×10^3 and 150×10^3, and the results were compared with data obtained using a conventional hot-wire probe. Significant attenuation was observed in the hot-wire results even with wires as short as 7 viscous units for all wavenumbers greater than, and including, the energy-containing motions.

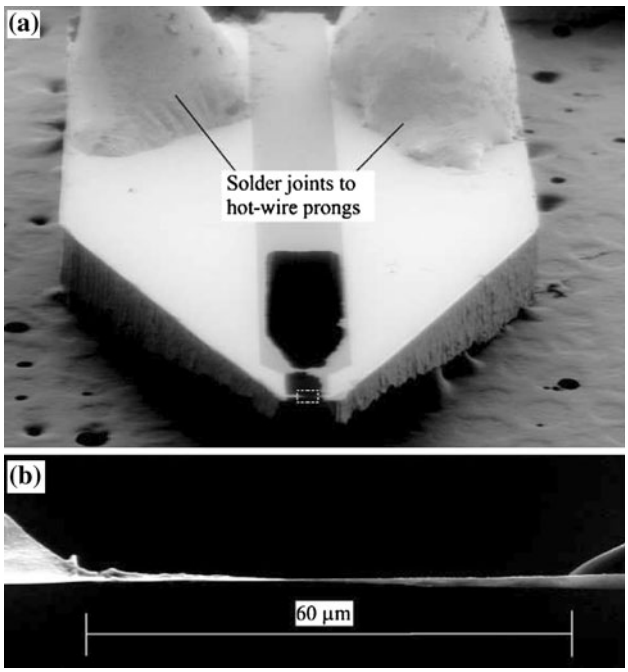

Fig. 1 Scanning electron microscope image of the original NSTAP design used by Bailey et al. (2010) showing (**a**) the whole probe and (**b**) close-up of region indicated by *dashed box* showing wire sensing length

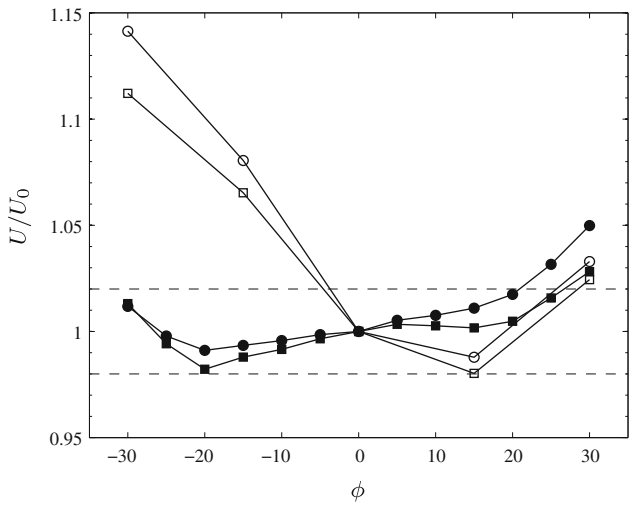

Fig. 2 Sensitivity of the NSTAP to pitch angle. Original NSTAP design (*hollow symbols*), new NSTAP design (*filled symbols*) at *open circle*, 10 m/s; *open square*, 20 m/s. *Dashed lines* show ±2% variation limits. Positive angles correspond to the metal side of the NSTAP facing the flow and negative to the silicon side facing the flow

2 Probe design

The process used to manufacture of the new design NSTAP is similar to that described in Bailey et al. (2010), using a range of conventional semiconductor fabrication techniques. A double-side-polished silicon wafer is first covered with silicon oxide on one side. Using photolithography and electron-beam evaporation, a thin metal layer (10 nm Ti and 100 nm Pt) with the probe pattern is deposited onto the oxide layer. The probe pattern is shown in Fig. 3, where the sensing element is shown having dimensions 60 μm × 2 μm with a thickness determined by the metal layer (100 nm).

To construct a three-dimensional streamlined structure with smoothly decreasing thickness, the deep reactive ion etching (DRIE) technique together with RIE lag has been implemented, instead of the laser machining approach used by Bailey et al. (2010). DRIE, first introduced by Bosch (Laermer and Schilp 1996), is a highly anisotropic etch process used for generating high-aspect-ratio holes and trenches in silicon substrates. The Bosch process is mainly used for creating vertical walls, but in order to generate smoothly sloping surfaces, we took advantage of aspect-ratio-dependent etching, known as RIE lag. Chung (2004) investigated the effect of pattern geometry on RIE lag, and Rao et al. (2004) describe microfabrication of complex, high-aspect-ratio structures with arbitrary surface height profiles in bulk silicon by making use of RIE lag. Our approach, DRIE lag, is less complicated, allowing all the etching to be done without intermediate thermal oxidation or wet etching steps, and it is more similar to that described by Chou and Najafi (2002). Using photolithography (Fig. 4a), we first etch trenches with different depths simultaneously, leaving 5-μm-thick sidewalls between individual gaps, as shown in Fig. 4b. A short isotropic etch is then used to remove the sidewalls and smooth the surface (Fig. 4d), resulting in the desired tapered silicon structure. This process is done on the backside of the wafer, by matching the pattern on the front side using a backside mask aligner. The mask allows the etching of the probes into the desired three-dimensional shape and releases individual probes from the wafer, leaving them freestanding. This novel DRIE lag process also has advantages for batch manufacturing over laser machining, where every probe needs to be shaped individually. Freestanding probes are then soldered onto conventional hot-wire prongs allowing the use NSTAPs in the same experimental apparatus used for conventional hot-wires. Finally, a short buffered oxide etch is done on every probe separately to remove the underlying silicon oxide, which results in aerodynamically shaped probes with freestanding 60 μm × 2 μm × 100 nm sensing elements, as shown in Fig. 5.

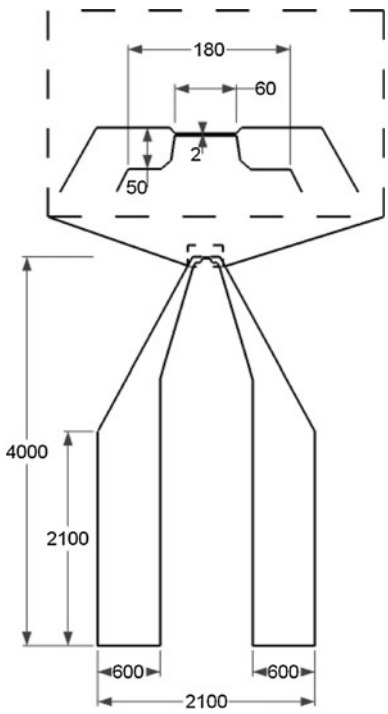

Fig. 3 Pattern sketch of the new NSTAP design metal structure with a zoomed view of the sensing element. All measurements given in μm

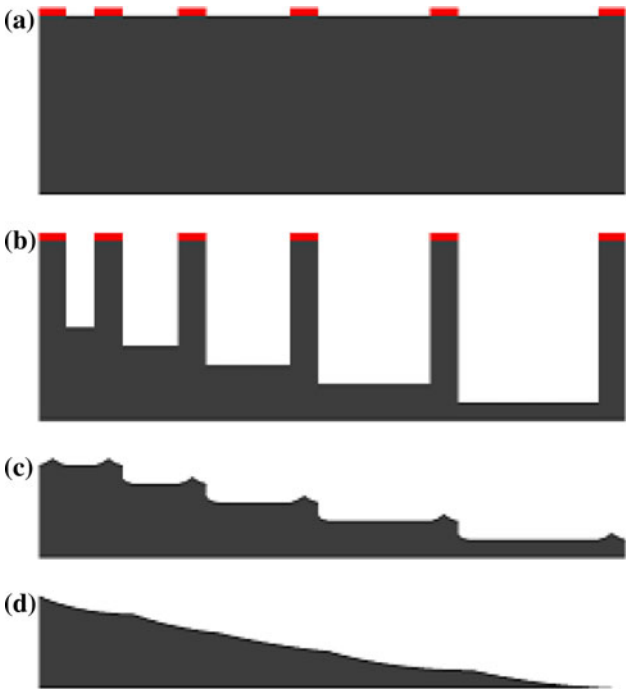

Fig. 4 Schematic representations of the DRIE-lag-based process flow. **a** Photolithography; **b** Bosch etching of the substrate; **c** Removal of the sidewalls by isotropic etch; **d** Anisotropic etch for smoothing the surface. *Gray* indicates silicon, *red* indicates photoresist

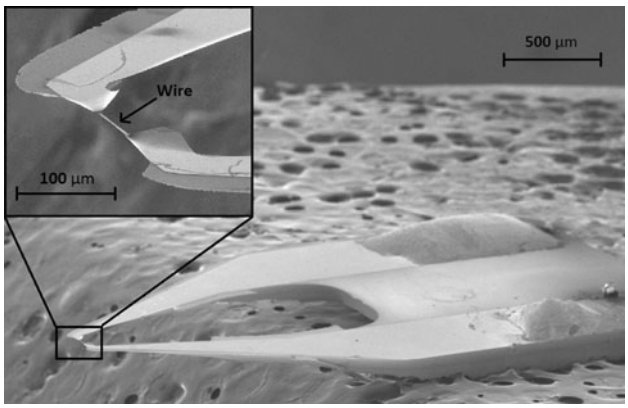

Fig. 5 Scanning electron microscope images of a typical 60-μm new NSTAP design. The probe is mounted on a wax substrate (seen in the background) for imaging

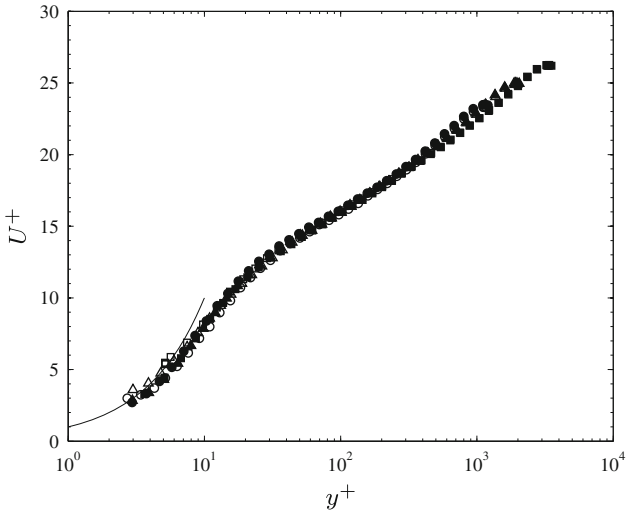

Fig. 6 Mean velocity profiles in inner variables measured with the new NSTAP (*filled symbols*) and conventional hot-wire (*hollow symbols*) at *open circle*, $Re_D = 45{,}000$; *open triangle;* $Re_D = 80{,}000$; *open square*, $Re_D = 150{,}000$. The *solid line* indicates linear region where $U^+ = y^+$

3 Experiment

Measurements of the streamwise component of the turbulence intensity and frequency spectra were obtained for Reynolds numbers Re_D ranging from 45×10^3 to 150×10^3, where $Re_D = \langle U \rangle D/\nu, D$ is the pipe diameter and $\langle U \rangle$ denotes the area-averaged velocity. The experiments were conducted in the Princeton University/ONR Superpipe, described in detail by Zagarola (1996) and Zagarola and Smits (1998). Even though the facility can be pressurized, all experiments presented here were conducted at atmospheric pressure. The pipe was a commercial steel pipe with an average inner diameter of 129.84 mm and an overall length of 196 D. The friction velocity u_τ was found from the pressure drop along the pipe. The mean flow behavior is described by Langelandsvik et al. (2007), who showed that the pipe is hydraulically smooth for $Re_D < 8 \times 10^5$.

As described in the previous section, the NSTAP sensor measured 60 μm × 2 μm × 100 nm. The hot-wire probe was of a conventional design with a sensor length of 0.4 mm and diameter of 2.5 μm, made of Wollaston wire (90% Pt, 10% Rh). The NSTAP and hot-wire were operated in the constant temperature mode at resistance overheat ratios of 1.3 and 1.5, respectively. A commercial hot-wire system was operated with a 1:1 bridge and external resistor (Streamline, Dantec Dynamics A/S, Denmark). The square wave test indicated frequency response above 40 kHz for the hot-wire and 150 kHz for the NSTAP. The measurements were taken at sampling rates of 60 and 300 kHz, for hot-wire and NSTAP, respectively, and low-pass filtered using a fourth-order Butterworth filter at half the sampling rate, always greater than the local Kolmogorov frequency. The initial location of each sensor was determined using a z-axis measuring microscope (Titan Tools ZDM-1) with an accuracy of ±3 μm. The traverse encoder had an accuracy of ±3 μm/m, and the resolution was 5 and 1 μm for hot-wire and NSTAP setup, respectively. The experimental conditions for all cases studied are summarized in Table 1, where $Re_\tau = Ru_\tau/\nu$ and y_0 is the initial wall-normal position of the probe.

To obtain the pitch sensitivity results shown in Fig. 2, the NSTAP was placed in a 0.6 m × 0.9 m closed-circuit wind tunnel. The probe was calibrated at pitch angle $\varphi = 0$, and the angular sensitivity of the probe was evaluated by pitching the probe in the range of $-60 < \varphi < 60$ at two different free-stream velocities, 10 and 20 m/s.

Table 1 Experimental conditions

Case	Probe	Re_D	Re_τ	$\langle U \rangle$ (ms^{-1})	l_w^+	y_0 (μm)
1	Hot-wire	42,300	1,137	4.95	7.0	80
2		78,400	1,942	9.19	12.0	80
3		144,000	3,337	17.0	20.6	100
4	NSTAP	42,700	1,133	5.00	1.0	27
5		77,900	1,923	9.19	1.8	28
6		143,000	3,312	16.9	3.1	28

4 Results

Figure 6 shows the mean velocity profiles for all cases in inner variables, where $U^+ = \overline{U}/u_\tau$ and $y^+ = yu_\tau/\nu$. The hot-wire and NSTAP data show excellent agreement for all three Reynolds numbers. Some slight differences can be seen in the hot-wire data at small y^+, due to the fact that the accuracy in determining the wall position for NSTAP probes is better than for hot-wire probes (depending on traverse resolution).

Figure 7 shows distributions of the streamwise variance $u^{+2} = \overline{u^2}/u_\tau^2$. It can be seen that in the outer flow for all three Reynolds numbers, the NSTAP data agree remarkably

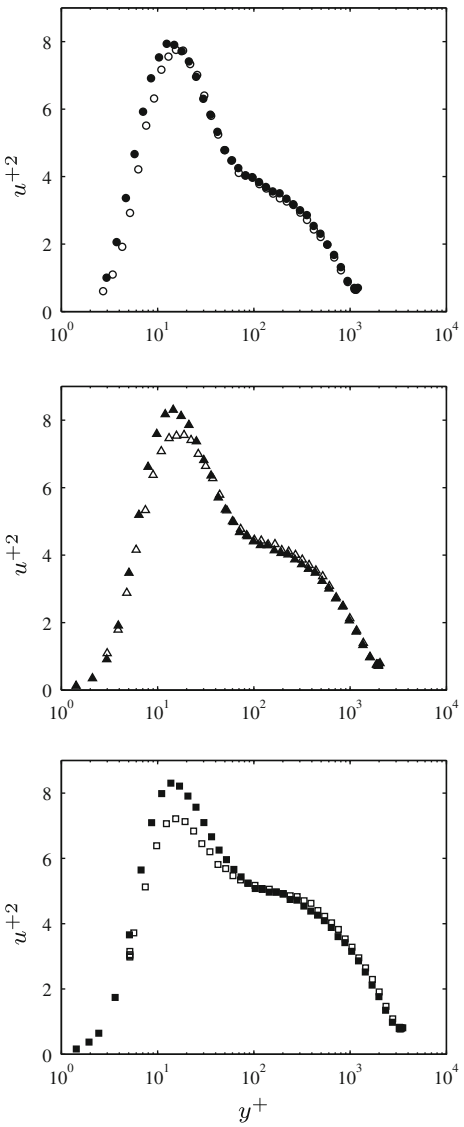

Fig. 7 Streamwise turbulence intensity profiles measured with NSTAP (*filled symbols*) and conventional hot-wire (*hollow symbols*) at *open circle*, Re_D = 45,000, *open triangle*, Re_D = 80,000; *open square*, Re_D = 150,000

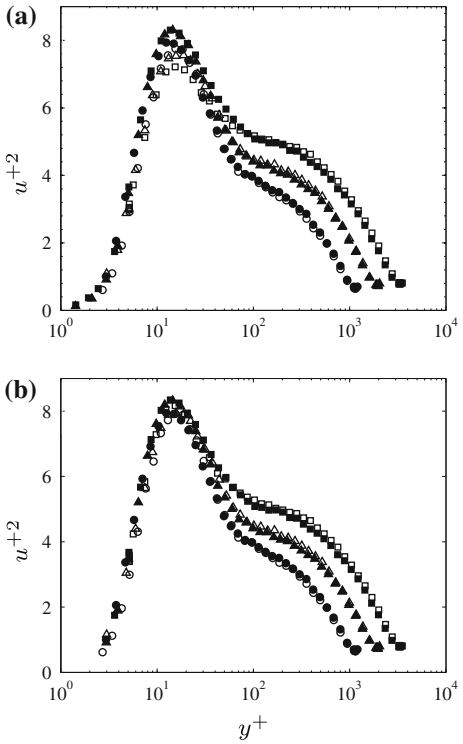

Fig. 8 Streamwise turbulence intensity profiles **a** uncorrected and **b** corrected for spatial filtering; measured with NSTAP (*filled symbols*) and conventional hot-wire (*hollow symbols*) at *open circle*, Re_D = 45,000; *open triangle*, Re_D = 80,000; *open square*, Re_D = 150,000

well with the hot-wire data, and an inner peak in intensity at $y^+ \approx 15$ is seen in each profile. However, discrepancies due to spatial filtering are observed in the near-wall region, increasing with Reynolds number. That is, discrepancies are seen for $y^+ < 15$ at $Re_D = 45{,}000$, $y^+ < 25$ at $Re_D = 80{,}000$ and $y^+ < 50$ at $Re_D = 150{,}000$. For the NSTAPs, where $1.0 \leq l_w^+ \leq 3.1$, the profiles agree in every respect at each Reynolds number (as can be seen in Fig. 8a), demonstrating that no significant spatial filtering effects are present in the NSTAP data. However, for the hot-wire data, where $7 \leq l_w^+ \leq 20.6$, some filtering is evident even at the lowest Reynolds number in the region $y^+ < 15$.

To allow for the effects of spatial filtering, Smits et al. (2011) developed a correction for u^{+2} based on the near-wall peak correction suggested by Hutchins et al. (2009) and the attached eddy hypothesis to account for spatial filtering effects at more distant wall-normal positions. In Fig. 8a, the turbulence intensity distributions are shown without this correction, and in Fig. 8b, they are shown with this correction applied. The corrected hot-wire and NSTAP data collapse onto a single curve for each Reynolds number, and for $y^+ \leq 20$, the data show a universal behavior with a peak value $u^{+2} = 8.1 \pm 0.2$. These results demonstrate the accuracy of the correction method

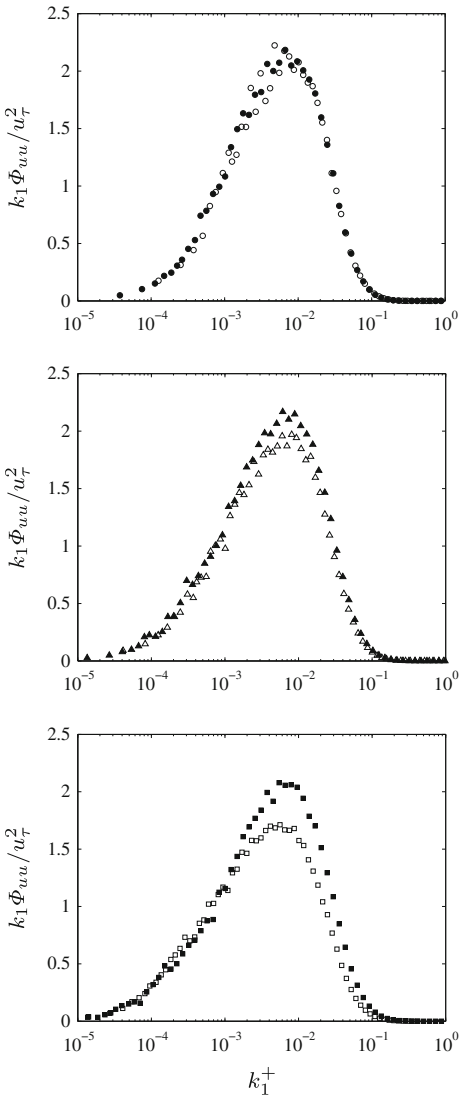

Fig. 9 Premultiplied energy spectra of the streamwise velocity signal at the location of the inner peak; measured with NSTAP (*filled symbols*) and conventional hot-wire (*hollow symbols*) at *open circle*, Re_D = 45,000; *open triangle*, Re_D = 80,000; *open square*, Re_D = 150,000

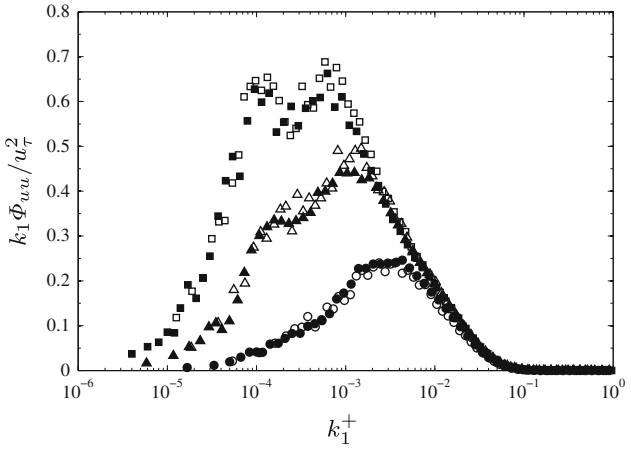

Fig. 10 Premultiplied energy spectra of the streamwise velocity signal in outer region at $y^+ = 1{,}000$; measured with NSTAP (*filled symbols*) and conventional hot-wire (*hollow symbols*) at *open circle*, Re_D = 45,000; *open triangle*, Re_D = 80,000; *open square*, Re_D = 150,000

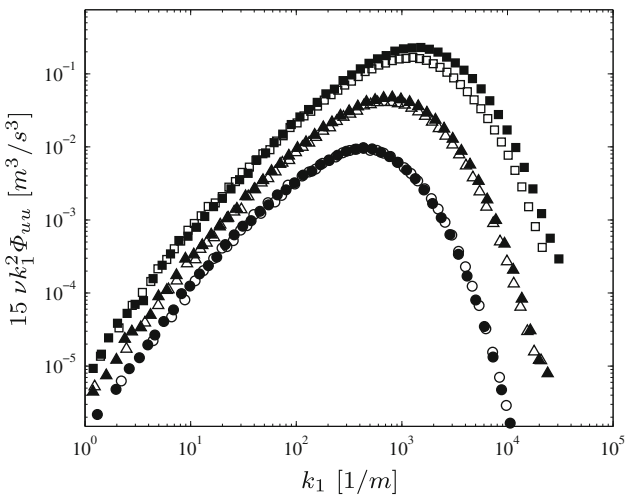

Fig. 11 Measured dissipation spectra at $y^+ = 15$; measured with NSTAP (*filled symbols*) and conventional hot-wire (*hollow symbols*) at *open circle*, Re_D = 45,000; *open triangle*, Re_D = 80,000; *open square*, Re_D = 150,000

proposed by Smits et al. (2011), and they also reinforce the conclusions made by Hultmark et al. (2010) regarding the invariance of the peak intensity with Reynolds number in pipe flows.

In Fig. 9, the premultiplied one-dimensional streamwise energy spectra $k_1\Phi_{uu}$ are shown for the point closest to $y^+ = 15$, that is, the location where the peak in turbulence intensity occurs. At low wavenumbers, that is for $k_1^+ < 2 \times 10^{-3}$ (where $k_1^+ = k_1 \nu/u_\tau$, and k_1 is the streamwise wavenumber), the hot-wire and NSTAP data agree at each Reynolds number, although the energy content increases with increasing Reynolds number, as expected. At higher wavenumbers ($k_1^+ > 2 \times 10^{-3}$), the spectra show a clear influence of spatial filtering, with the hot-wire results consistently falling below the NSTAP results. This spatial filtering effect can have a significant effect on investigations of scaling behavior, such as the slope of the spectrum in the inertial region. Focusing on the NSTAP data alone, we see that the slight decrease in the peak values of the spectra near $k_1^+ = 8 \times 10^{-3}$ with increasing Reynolds number is balanced by a similar increase at larger wavenumbers, thereby keeping the total energy content constant. This result agrees with the earlier observations by Hultmark et al. (2010).

Further from the wall, the spatial filtering effects are much reduced and the hot-wire and NSTAP show excellent

agreement. This may be seen in Fig. 10 where the premultiplied spectra are shown for $y^+ = 1{,}000$.

The dissipation spectra, estimated from $15\nu k_1^2 \Phi_{uu}$ at $y^+ = 15$, are shown in Fig. 11. For $Re_D = 45 \times 10^3$, there is excellent agreement between the two probes, but at higher Reynolds numbers, the NSTAP measures a higher dissipation rate than the hot-wire, again as a result of spatial filtering effects on the hot-wire data at higher Reynolds numbers.

5 Conclusions

A new, more streamlined nano-scale thermal anemometry probe (NSTAP) has been developed using an innovative manufacturing process. Measurements of the streamwise component of velocity were performed in fully developed turbulent pipe flow and compared with the data obtained using a conventional hot-wire probe. The mean flow results showed excellent agreement, but the turbulence intensity distributions and frequency spectra show that the hot-wire results suffer from spatial filtering effects, even for probes as short as 7 viscous units. In contrast, the NSTAP results showed no detectable effects of spatial filtering. These effects are particularly important for estimating the height of the near-wall peak in the streamwise turbulence intensity distribution and the distribution of energy among wavenumbers.

Acknowledgments The support provided by ONR through Grant N00014-9-1-0138 (Program Manager Dr. Ron Joslin) is gratefully acknowledged. Authors would also like to acknowledge George Patrick Watson of the PRISM Micro/Nano Fabrication Laboratory at Princeton University for his invaluable advice and assistance in developing the NSTAP fabrication process and Jim Sturm, the Director of PRISM, for making the microfabrication facilities available.

References

Bailey SC, Hultmark M, Schumacher J, Yakhot V, Smits AJ (2009) Measurements of the dissipation scales in turbulent pipe flow. Phys Rev Lett 103:103–014,502

Bailey SCC, Kunkel GJ, Hultmark M, Vallikivi M, Hill JP, Meyer KA, Tsay C, Arnold CB, Smits AJ (2010) Turbulence measurements using a nanoscale thermal anemometry probe. J Fluid Mech 663:160–179

Cameron JD, Morris SC, Bailey SCC, Smits AJ (2010) Effects of hot-wire length on the measurement of turbulent spectra in anisotropic flows. Meas Sci Technol 21:105407

Chin CC, Hutchins N, Ooi AS, Marusic I (2009) Use of direct numerical simulation (DNS) data to investigate spatial resolution issues in measurements of wall-bounded turbulence. Meas Sci Technol 20:115,401

Chou TKA, Najafi K (2002) Fabrication of out-of-plane curved surfaces in Si by utilizing RIE lag. In: Proceedings of 15th IEEE international conference on micro electro mechanical systems. pp 145–148

Chung CK (2004) Geometrical pattern effect on silicon deep etching by an inductively coupled plasma system. J Micromech Microeng 14:656–662

Comte-Bellot G (1976) Hot-wire anemometry. Ann Rev Fluid Mech 8:209–231

Hultmark M, Bailey SCC, Smits AJ (2010) Scaling of near-wall turbulence in pipe flow. J Fluid Mech 649:103–113

Hutchins N, Nickels TB, Marusic I, Chong MS (2009) Hot-wire spatial resolution issues in wall-bounded turbulence. J Fluid Mech 635:103–136

Kim KC, Adrian RJ (1999) Very large-scale motion in the outer layer. Phys Fluids 11(2):417–422

Kolmogorov AN (1941) The local structure of turbulence in incompressible viscous fluid for very large Reynolds numbers. Dokl Akad Nauk SSSR 30:301–305, reprinted in 1991: Proc. R. Soc. Lond. A, 434, 9–13

Laermer F, Schilp A (1996) Method for anisotropic plasma etching of substrates. Patent #5498312

Langelandsvik LI, Kunkel GJ, Smits AJ (2007) Flow in a commercial steel pipe. J Fluid Mech 595(323-339):323–339

Ligrani PM, Bradshaw P (1987) Subminiature hot-wire sensors: development and use. J Phys E Sci Instrum 20:323–332

Perry AE, Henbest SM, Chong MS (1986) A theoretical and experimental study of wall turbulence. J Fluid Mech 165:163–199

Rao MP, Aimi MF, MacDonald NC (2004) Single-mask, three-dimensional microfabrication of high-aspect-ratio structures in bulk silicon using reactive ion etching lag and sacrificial oxidation. App Phys Lett 85-25:6281–6283

Smits AJ, Monty J, Hultmark M, Bailey SCC, Hutchins M, Marusic I (2011) Spatial resolution correction for wall-bounded turbulence measurements. J Fluid Mech 676:41–53

Zagarola MV (1996) Mean-flow scaling of turbulent pipe flow. PhD thesis, Princeton University

Zagarola MV, Smits AJ (1998) Mean-flow scaling of turbulent pipe flow. J Fluid Mech 373:33–79